JOURNAL OF MATERIALS SCIENCE 30 (1995) 5130–5138

Thermal decomposition of ferric and ammonium sulphates obtained by bio-oxidation of water pickling liquors with *Thiobacillus ferrooxidans*

A. LOPEZ-DELGADO, F. A. LOPEZ
Department of Materials Recycling, National Center of Metallurgical Research (CSIC), Avda, Gregorio del Amo 8, E-28040 Madrid, Spain

Sulphuric water pickling liquor containing ferrous sulphates was oxidized by *Thiobacillus ferrooxidans* at different pHs. The oxidized solution was then evaporated and crystallized, and products characterized by X-ray powder diffraction, X-ray high temperature powder diffraction and Fourier transform infrared (FTIR) spectrometry. The thermal decomposition of these materials, studied by calorimetric and thermogravimetric techniques, shows that iron(III) hydroxysalts and monoammonium and triammonium salts are formed during the oxidation–evaporation–crystallization process. However, this formation depends upon pH.

1. Introduction

The pickling of carbon steel, performed with either sulphuric or hydrochloric acids, involves the elimination of superficial metallic oxides by immersion of metals in hot acidic solutions. Pickling may also be used in steel finishing processes, such as cold rolling, galvanizing, tin plating and enamelling of semifinished steel.

Significant pollutants in water pickling liquor (WPL) include suspended solids, total iron, ferrous iron, dissolved iron and acids. Pickling liquor is listed as hazardous waste in the US Resource Conservation and Recovery Act (US RCRA, Public Law 94–580) because of its corrosive properties [1].

Technologies for treating these hazardous effluents are required.

In previous papers [2, 3] preliminary work with these solutions was reported and the possibility of using *Thiobacillus ferrooxidans* in the treatment of waste generated by iron making and steelmaking was demonstrated.

With respect to the oxidation of ferrous sulphate solutions in ammonium containing media by these organisms, several studies have been reported in the literature [4, 5].

According to Toro *et al.* [6] the mechanism of oxidation of ferrous solutions may be described in four stages.

1. Bacterial oxidation, giving rise to the formation of Fe^{3+} in solution with an increase in pH as a consequence of consumption of H^+ ions.
2. A fall in pH accompanied by the formation of an active amorphous precipitate of $Fe(OH)_3$, while the concentrations of ammonium and sulphate ions in solution remain constant. The fall in pH during bacterial oxidation has been amply described [6, 7].
3. A decrease in ammonium and sulphate concentrations and the continued fall in pH along with the appearance of precipitates of hydroxysalts. Normally, the formation of these compounds takes place at pHs between 1.9 and 2.2 [7, 8].
4. In the fourth and final stage there is an absence of ferrous ions indicating that oxidation has been completed.

This paper reports an investigation into the compounds formed when these bacterially treated solutions are evaporated and crystallized. No previous investigation of this type has been made.

Sulphuric WPL containing ferrous sulphate was oxidized by *Thiobacillus ferrooxidans*, evaporated and crystallized and the products characterized. Bacterial oxidation was performed at different pHs in a medium containing ammonium ions. The influence of pH on the production of iron(III) and ammonium salts and hydroxysalts was investigated and a possible explanation for the production of these compounds is offered. The thermal decomposition of these materials was also investigated.

2. Experimental procedure

Water pickling liquor (WPL) was collected from line No. 2 of the Ensidesa pickling plant (Avilés, Spain). Its composition, determined by titration, was 145.2 g $FeSO_4\,l^{-1}$ and 93.6 g $H_2SO_4\,l^{-1}$. Traces of ferric iron and chlorides were also present. For bacterial culture, the WPL sample was diluted with distilled water in the ratio of one part WPL to nine parts water, and pH was adjusted to 1.60, 1.75 and 2 by adding 50, 64 and 70 ml of 2.5 M $NH_4OH\,l^{-1}$, respectively. The *Thiobacillus ferrooxidans* used in this investigation was a laboratory strain cultivated in 'nine K' medium

0022–2461 © *1995 Chapman & Hall*

[9]. Microorganisms were adapted to pHs of less than two (but always within their life limits [3]). The bio-oxidation process was performed in a reactor at 31 °C using a 2% (v/v) bacterial inoculum. Samples for ion analysis were collected every 24 h. When the oxidation process was complete (after three days) the solutions obtained were filtered to remove microorganisms using a Millipore amicrobic filter. Solutions were then concentrated and crystallized by evaporation at 100 °C for 24 h.

The solids obtained were characterized by X-ray powder diffraction (XRD) employing a Siemens D-500 diffractometer with monochromatized CuK_α radiation. Fourier-transform Infrared (FT-IR) spectra were recorded in the 4000–400 cm^{-1} region using a Nicolet 550 spectrometer in transmission mode. Samples were prepared by mixing with ICs. Calorimetric studies were performed up to 750 °C using a Shimazdu DSC 50 differential scanning calorimeter (DSC). Thermogravimetric (TGA) curves were obtained up to 1100 °C using a Shimazdu TGA-50H instrument. Samples of about 15 mg were used in each test. All samples were decomposed in flowing air (20 ml min^{-1}) and at a heating rate of 20 °C min^{-1}. X-ray high temperature diffraction studies were carried out *in vacuo* (0.2 MPa) using an Anton Paar HTK10 heating chamber coupled to a Philips PW 1310 X-ray diffractometer. Data were collected after maintaining samples at 375, 425 and 500 °C for 15 min.

3. Results

3.1. X-ray powder diffraction and FTIR studies

Fig. 1 shows the XRD patterns of samples obtained at different pHs. The crystalline phases observed are Fe(III) and ammonium salts and hydroxysalts. At pH 1.6, the principal crystalline phase consists of $NH_4Fe(SO_4)_2$. Secondary crystalline phases are $(NH_4)_3Fe(SO_4)_3$ and $(NH_4)_2SO_4 \cdot Fe_2(SO_4)_3$. At pH 1.75 the diffractogram shows a fall in the relative intensity of peaks corresponding to $(NH_4)Fe(SO_4)_2$ as the concentrations of $(NH_4)SO_4 \cdot Fe_2(SO_4)_3$ and $(NH_4)_3Fe(SO_4)_3$ begin to increase. At pH 2, peaks corresponding to $(NH_4)Fe(SO_4)_2$ are not observed. At this pH the crystalline phase is composed of $(NH_4)_3Fe(SO_4)_3$ and $(NH_4)_2SO_4 \cdot Fe_2(SO_4)_3$ along with Fe(III) hydroxysalts. Those that can be identified in the diffractogram are $Fe_4(OH)_{10}SO_4$, $Fe(OH)SO_4 \cdot 2H_2O$ and hydroniumjarosite $H_3OFe_3(OH)_6(SO_4)_2$.

Table I summarizes the assignment of the i.r. bands of these materials according to criteria used in other investigations [8–13]. Bands at 3447, 875 and 472 cm^{-1} that may be attributed to the OH group vibrations seen in Fe(III) hydroxysalts [10–12], are only observed in the i.r. spectrum of the solid obtained at pH 2. In this case, bands of weak intensity observed around 2808 and 2924 cm^{-1} could correspond to the vibrational modes $\upsilon_1(H_3O^+)$ and $\upsilon_3(H_3O^+)$ of hydroniumjarosite [11]. With respect to NH_4 and SO_4 groups, the slight displacement of bands corresponding to their vibrational modes could be due to salts of different composition within these materials.

3.2. Thermal studies

DSC, TGA and derivated TGA (DvTGA) curves recorded for solids obtained at pH 1.6, 1.75 and 2 are shown in Fig. 2a–c, respectively. Several differences in thermal decomposition are observed.

TGA curves show that the decomposition process in solids obtained at pH 1.6 and 1.75 occurs in three well-defined steps. The first takes place between approximately 250 and 440 °C with a weight loss of 14.70 for material obtained at pH 1.6, and 16.95% for material obtained at pH 1.75. This is reflected by two endothermic peaks. A second step occurs between approximately 440 and 550 °C with a weight loss of 18.47 for material obtained at pH 1.6 and 20.20% for material obtained at pH 1.75. Finally, between approximately 600 and 725 °C, weight losses of 33.82 and 35.30% take place in samples obtained at pH 1.6 and 1.75, respectively. The two last steps are reflected by one endothermic peak in each case.

In solids obtained at pH 2, a weight loss of 54.88% occurs between 200 and 550 °C in two steps that are not so well defined. The first is reflected by four endothermic peaks (Fig. 3c). Finally, between 550 and 750 °C, a last step takes place with a weight loss of 21.46%.

In the DSC curve of this solid, the first and the second peak, seen at 234 and 283 °C, peak temperature, T_p, and not observed at pHs below 2, could correspond to the dehydroxylation of hydroxysalts [14]. The dehydroxylation reactions could produce oxysulphates as shown in the generic reaction below

$$Fe_x(OH)_y(SO_4)_z + \tfrac{1}{4}y\,O_2 \rightarrow \tfrac{1}{2}y\,H_2O + Fe_xO_y(SO_4)_z \quad (1)$$

Table II summarizes the transformation energy corresponding to each decomposition process. These values are calculated by integration of DSC peaks and the maximum temperature of each peak. The transformation energy associated with the decomposition reactions (corresponding to the endothermic peak observed in all materials between 270 and 378 °C) increases as pH rises. There is also a pH associated displacement of the temperature of the peak. As pH increases, temperature increases. This peak could correspond to the thermal degradation of $(NH_4)_2SO_4 \cdot Fe_2(SO_4)_3$ shown by the following equation

$$(NH_4)_2SO_4 \cdot Fe_2(SO_4)_3 \rightarrow 2(NH_4)\,Fe(SO_4)_2 \quad (2)$$

The energy associated with this transformation reaction varies from 2.8 kJ kg^{-1} at pH 1.6 to 62 kJ kg^{-1} at pH 2. This is in agreement with XRD analyses that show this phase is a minority component at pH 1.6. DvTGA curves indicate that there is no loss of weight.

X-ray powder patterns recorded on samples obtained at pH 2, heated at 350 °C (Fig. 3a), show the disappearance of peaks corresponding to basic Fe(III) sulphates. At the same time, clear d_{hkl} peaks of $(NH_4)Fe(SO_4)_2$ appear. These are due to the decomposition of the remainder of the salt $(NH_4)_2SO_4 \cdot Fe_2(SO_4)_3$. There are also peaks that may be attributed to different Fe(III) oxysulphates.

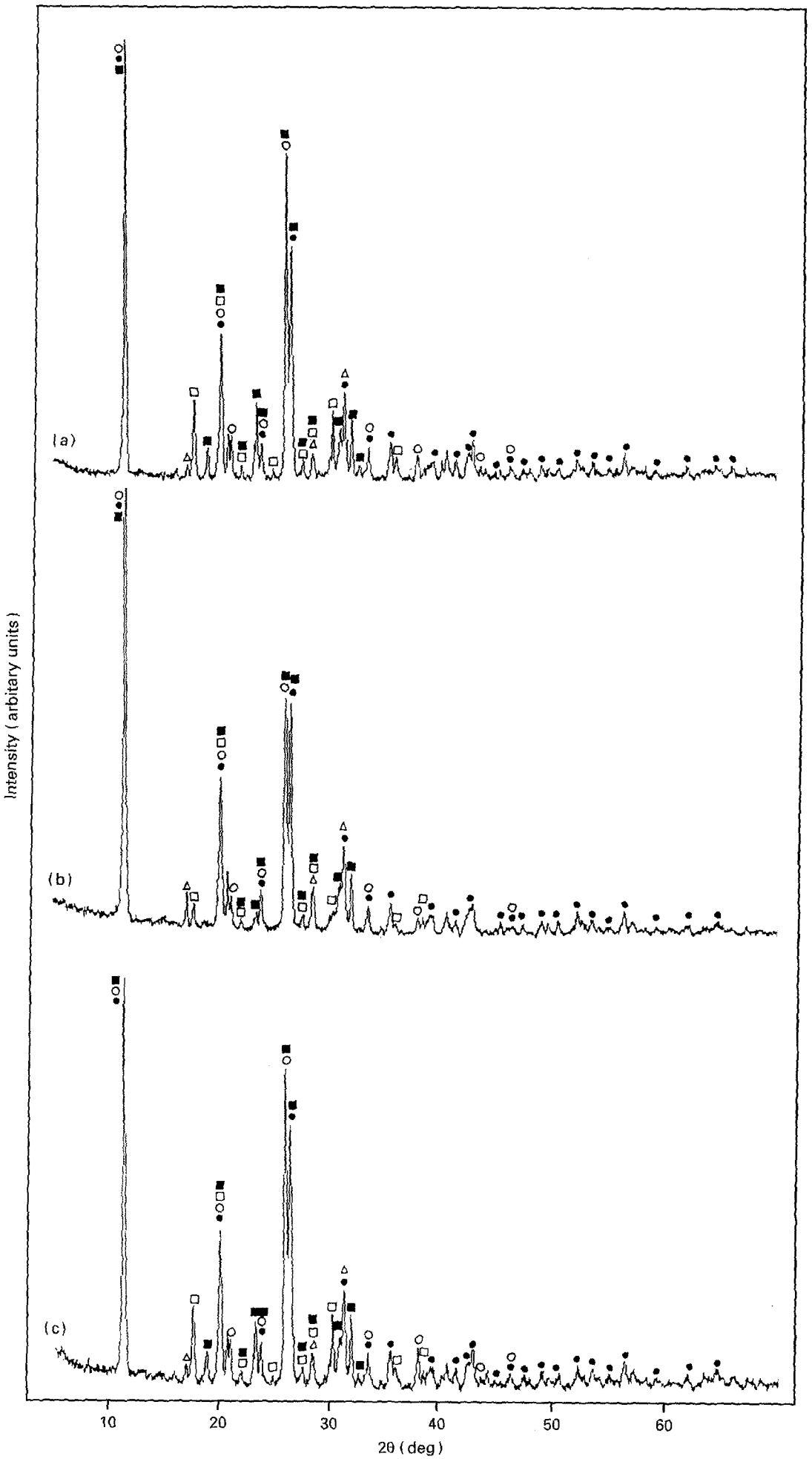

Figure 1 XRD patterns of the materials obtained at a dilution of 1:10 (v/v) with respect to pH. (a) pH 1.6, (b) pH 1.75, and (c) pH 2. (●) $(NH_4)_3Fe(SO_4)_3$, (○) $(NH_4)_2SO_4 \cdot Fe_2(SO_4)_3$, (□) $Fe(SO_4)OH \cdot 2H_2O$, (△) $(H_3O)Fe_3(SO_4)_2(OH)_6$, (■) $Fe_4(SO_4)(OH)_{10}$, (▲) $NH_4Fe(SO_4)_2$.

TABLE I I.r. absorbances observed of iron and ammonium salts from bacterial oxidized iron solutions

pH	OH st[a]	NH st	H_3O^+ st	H_2O df[b]	NH_4 df	υ_3SO_4	υ_1SO_4	OH df	υ_4SO_4	τOH	$\upsilon_2(SO_4)$	Other bands
1.60	–	3322 m[c] 3207 s[d], b[e] 3080 sh[f] 3030 w[g]	–	–	1472 sh 1428 w 1411 m	1246 s 1174 m 1084 sh 1057 sh 1030 vs[i]	866 m	–	656 m 595 m	–	449 m	323 sh 276 s 228 m
1.75	–	3323 m 3295 s, b 3088 w	–	–	1472 sh 1429 m	1242 sh 1174 hs 1113 vs 1056 sh	1011 vs	–	675 sh 656 m 598 m	470 sh	449 w	323 sh 275 sh 265 sh 252 m 228 m
2.00	3447 sh	3238 s, b 3085 m	2924 vw[h] 2857 vw	1690 vw	1429 s	1175 s 1115 vs	1009 vs	875 vw	678 w 599 s	472 w	449 w	323 m 279 m 254 m 228 m

[a] st, stretch; [b] df, deformation; [c] m, medium; [d] s, strong; [e] b, broad; [f] sh, shoulder; [g] w, weak; [h] vw, very weak; [i] vs, very strong.

The next endothermic peak in the DSC curves, corresponds to the decomposition of the sulphate $(NH_4)_3Fe(SO_4)_3$ in the following manner

$$2(NH_4)_3Fe(SO_4)_3 \rightarrow 6NH_3(g) + Fe_2(SO_4)_3 + 3H_2SO_4 \quad (3)$$

Here, the temperature of the peak also increases with rising pH (Table II). The energy associated with the transformation varies from 111 kJ kg^{-1} at pH 1.6 to 293 kJ kg^{-1} at pH 2. These results indicate that the presence of this salt increases as does the pH of bio-oxidized solution. This is in agreement with results from XRD analysis of initial samples. In the X-ray diffractogram of samples obtained after heating to 450 °C (Fig. 3b), peaks corresponding to $(NH_4)_3Fe(SO_4)_3$ are no longer observed. This pattern shows the presence of $(NH_4)Fe(SO_4)_2$ along with anhydrous Fe(III) sulphates and/or oxysulphates.

The endothermic peak observed between 440 and 521 °C could correspond to the decomposition of $(NH_4)Fe(SO_4)_2$ according to the equation

$$2(NH_4)Fe(SO_4)_2 \rightarrow 2NH_3(g) + Fe_2(SO_4)_3 + H_2SO_4 \quad (4)$$

The energy associated with the decomposition reaction decreases as pH rises (Table II). These results show that this compound is found mostly at pH 1.6 and 1.75. The low energy level associated with the reaction at pH 2 and the initial XRD analysis, which shows that this phase is not observed in this solid, suggest that the salt, $(NH_4)Fe(SO_4)_2$, present comes from the thermal degradation of $(NH_4)SO_4 \cdot Fe_2(SO_4)_3$ (see Equation 2).

Finally, between 615 and 692 °C, decomposition occurs of the Fe(III) sulphate and oxysulphates formed during the decomposition reactions, leading to the formation of the final product αFe_2O_3. The energy associated with this decomposition reaction, is similar for pH 1.6 and 1.75. However, at pH 2 the value is much lower. This is a consequence of the lower content of ferric sulphate and/or oxysulphates. At 750 °C, the X-ray diffractogram (Fig. 3c) indicates the sole presence of hematite.

3.3. X-ray high temperature powder diffraction

In order to confirm the above results, X-ray high temperature powder diffraction studies were carried out on solids obtained as pH 2.

X-ray patterns recorded for samples heated at 275 °C (Fig. 4a) show diffraction maxima corresponding to $(NH_4)_3Fe(SO_4)_3$, $(NH_4)_2SO_4 \cdot Fe_2(SO_4)_3$ and $(NH_4)Fe(SO_4)_2$ which begins to form at this temperature. At 375 °C (Fig. 4b) all peaks coincide with the diffraction maxima of iron(III) oxysulphates $Fe_{12}O_3(SO_4)_{15}$ and $Fe_4O(SO_4)_5$. This result would seem to indicate that the decomposition of all the starting salts has occurred via the formation of oxysulphates. Since both oxysulphates show similar reticular spacing, this technique is unable to tell if one or both salts are present in the sample. At 425 °C the diffractogram shows the beginning of the formation of αFe_2O_3 alongside the still-present previous phases. At 500 °C the diffraction maxima corresponding to oxysulphates diminish while those of hematites increase (Fig. 4c).

4. Discussion

From the results it follows that oxidation of Fe(II) solutions by *Thiobacillus ferrooxidans*, followed by crystallization of the solution obtained, produces mainly double salts of iron(III) and ammonium with Fe(III) hydroxysalts appearing as pH approaches two.

The mechanism of formation of jarosite-type hydroxysalts is explained by Toro *et al.* [6] in the following reactions

$$Fe^{2+} + H^+ + \tfrac{1}{4}O_2 \rightarrow Fe^{3+} + \tfrac{1}{2}H_2O \quad (5)$$

$$Fe^{3+} + H_2O \rightarrow \tfrac{1}{2}Fe_2(OH)_2^{4+} + H^+ \quad (6)$$

$$\tfrac{1}{2}Fe_2(OH)_2^{4+} + 2H_2O \rightarrow Fe(OH)_3 + 2H^+ \quad (7)$$

$$Fe^{3+} + 2SO_4^{2-} \rightarrow Fe(SO_4)_2^- \quad (8)$$

$$Fe(OH)_3 + Fe(SO_4)_2^- + H_2O + \tfrac{2}{3}A^+ \rightarrow \tfrac{2}{3}A[Fe_3(SO_4)_2(OH)_6] + \tfrac{2}{3}SO_4^{2-} + H^+ \quad (9)$$

with the global reaction

$$Fe(OH)_3 + \tfrac{1}{3}SO_4^{2-} + Fe^{3+} + H_2O + \tfrac{2}{3}A^+ \rightarrow \tfrac{2}{3}A[Fe_3(SO_4)_2(OH)_6] + H^+ \quad (10)$$

This scheme implies the formation of jarosites as insoluble material in the oxidized solution taking place at pHs greater than 1.9 [6–8].

An alternative scheme can be put forward when there is no precipitation of hydroxysalts, nor great changes in pH. As the ferrous ions are oxidized producing $Fe_2(OH)_2^{4+}$ complexes, the production of hydroxysalts may begin as shown in Equation 11

$$\tfrac{1}{2}Fe_2(OH)_2^{4+} + SO_4^{2-} \rightarrow FeOHSO_4 \quad (11)$$

At the same time, the ferric ion formed may react with the sulphate and ammonium ions present in the solution to form salts as shown below

$$Fe^{3+} + 2SO_4^{2-} \rightarrow Fe(SO_4)_2^- \quad (12)$$

$$Fe(SO_4)_2^- + NH_4^+ \rightarrow (NH_4)\,Fe(SO_4)_2 \quad (13)$$

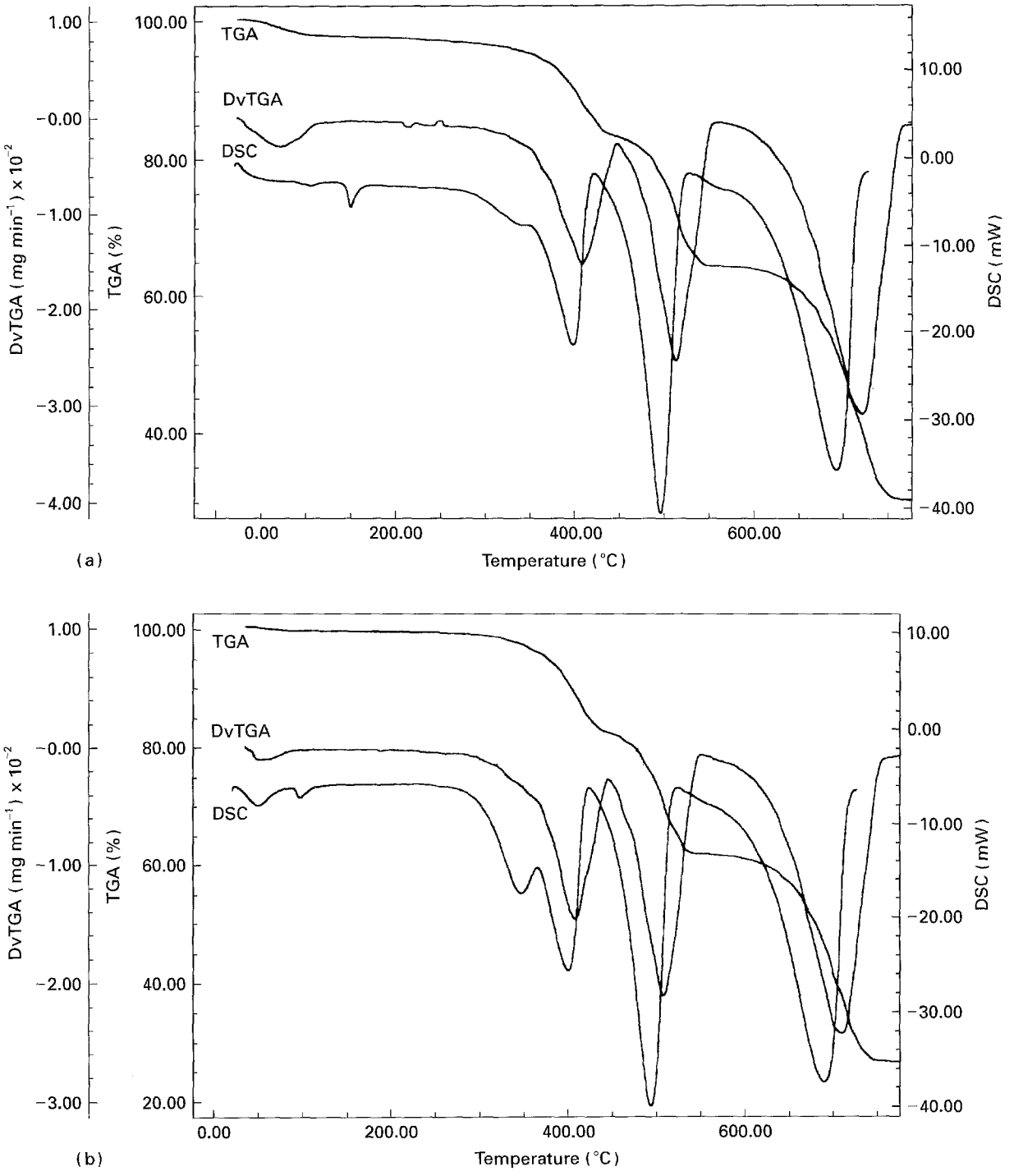

Figure 2 Differential scanning calorimetric (DSC), thermogravimetric (TGA) and its derivative (DvTGA) curves of the materials obtained with respect to pH: (a) 1.6, (b) 1.75, and (c) 2.

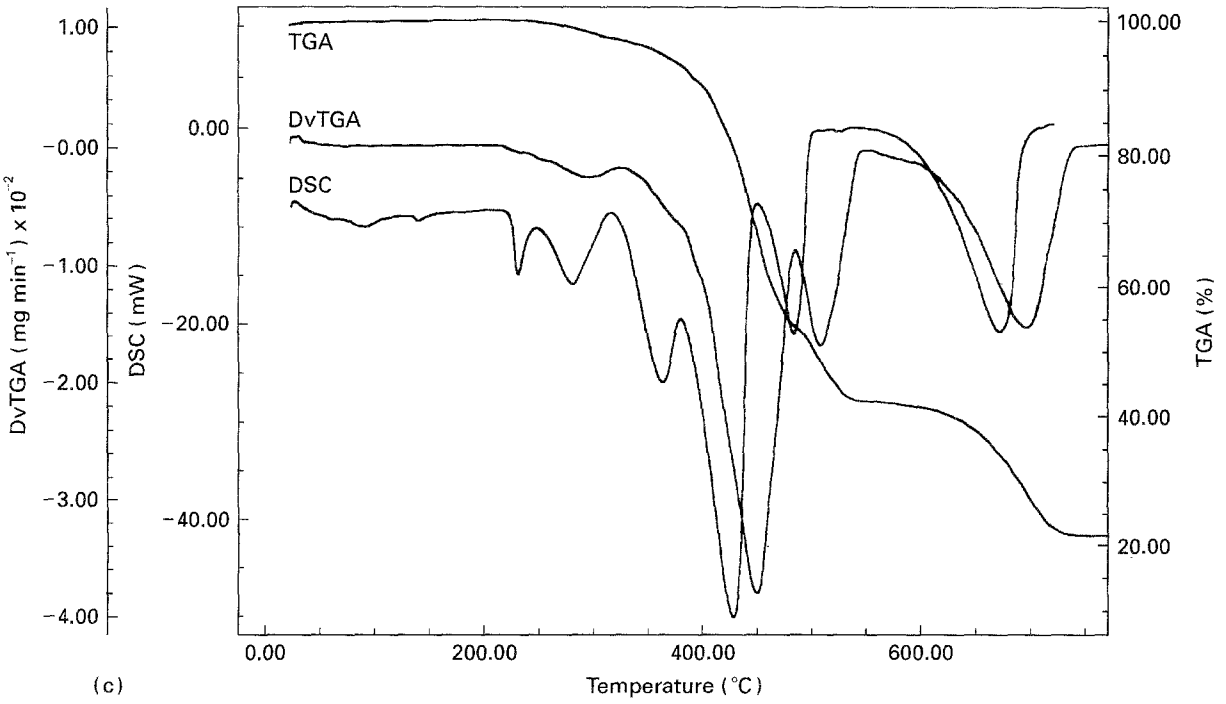

Figure 2 Continued.

TABLE II Phase changes from DSC plots at the different pHs

Process	pH 1.6		pH 1.75		pH 2.0	
	T_p[a] (°C)	Heat (kJ kg^{-1})	T_p (°C)	Heat (kJ kg^{-1})	T_p (°C)	Heat (kJ kg^{-1})
Dehydroxylation	–	–	–	–	234	13.1
					283	45.4
Thermal degradation of $(NH_4)_2SO_4 \cdot Fe_2(SO_4)_3$	284	2.8	346	32.1	366	62.0
Thermal decomposition of $(NH_4)_3Fe(SO_4)$	397	111.1	400	94.9	429	293.2
Thermal decomposition of $NH_4Fe(SO_4)_2$	496	303.4	494	272.4	486	98.2
Thermal decomposition of sulphates and oxysulphates	692	448.5	690	443.5	676	263.7

[a] T_p, peak temperature.

with the overall reaction

$$Fe^{3+} + 2SO_4^{2-} + NH_4^+ \rightarrow (NH_4)\,Fe(SO_4)_2 \quad (14)$$

To support this scheme of reactions the existence in solution of the species $Fe_2(OH)_2^{4+}$, $Fe(SO_4)_2^-$, $Fe(OH)_3$ and $Fe_2(SO_4)_3$ is necessary. The estimated values for ΔG° (kcal mol^{-1}) given in Table III clearly indicate the possible existence of these species in solution.

Therefore, the above mentioned salt and hydroxysalt can be formed from stable ions in solution. The other salts identified in the products are formed when the oxidized solution undergoes evapo–crystallization. This would be a consequence of the loss of water and the concurrent relative increase in the concentrations of (mainly) ammonium and sulphate ions. Therefore, it can be considered that during the evaporation of the solution, some of these salts would react in the presence of ammonium and sulphate ions to form the triammonium sulphate crystallized

$$(NH_4)Fe(SO_4)_2 + 2NH_4^+ + SO_4^{2-} \rightarrow (NH_4)_3Fe(SO_4)_3 \quad (15)$$

The results indicate that the concentration of this salt increases with increasing pH, coinciding with the greater concentration of ammonium ions in solution. With respect to the double salt $(NH_4)_2SO_4 \cdot Fe_2(SO_4)_3$, the results show that the proportion of this salt increases with increasing pH. Therefore, it may be that this salt forms, probably by a reaction between crystallized ferric sulphate and ammonium sulphate, as the solution evaporates and becomes relatively enriched in ammonium and sulphate ions.

The thermal decomposition of all the starting salts via the formation of $(NH_4)Fe(SO_4)_2$ and Fe(III) oxysulphates has been confirmed by X-ray high temperature studies. However, since these data were collected *in vacuo*, the formation temperatures of these phases

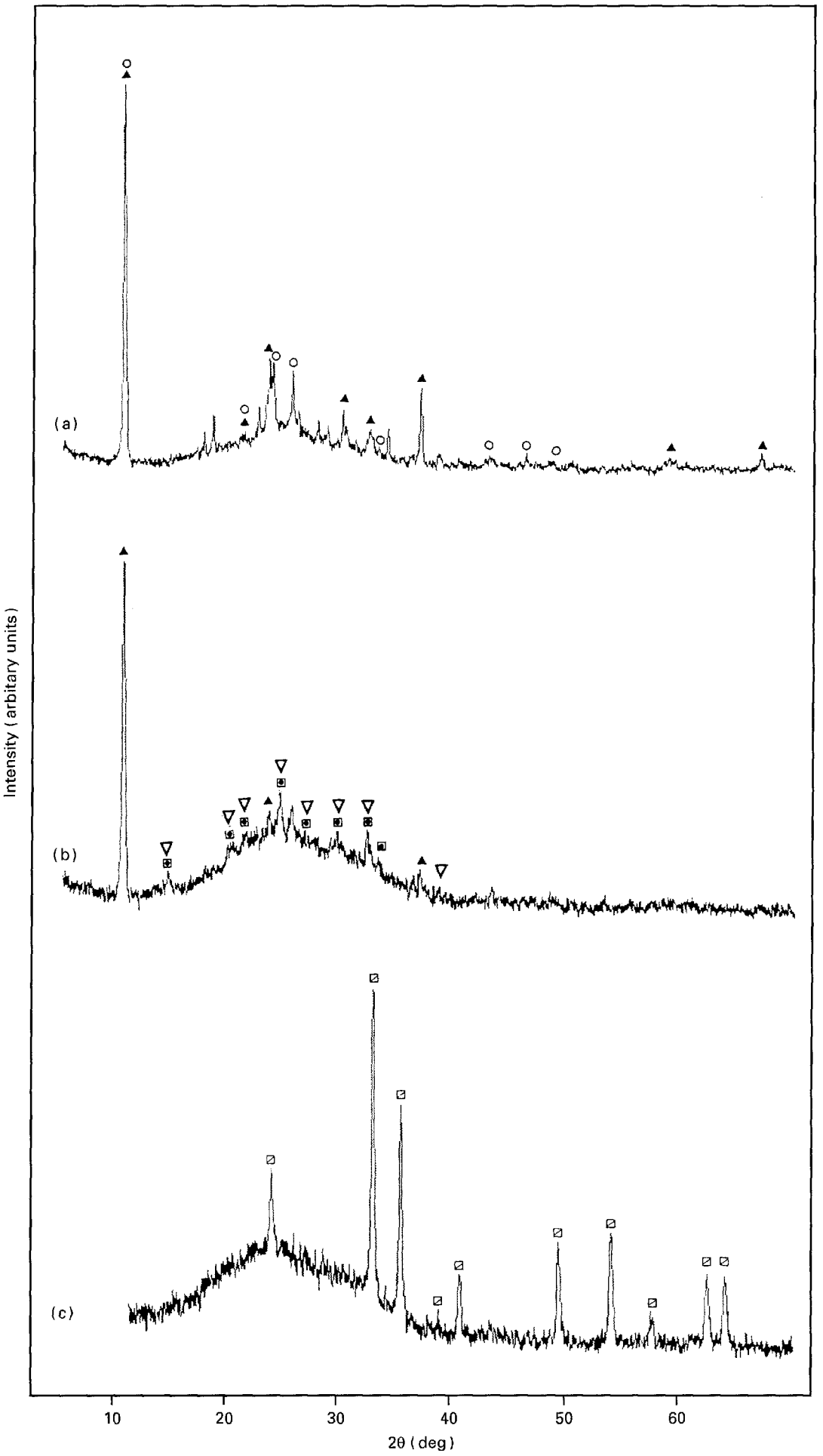

Figure 3 X-ray powder diffraction patterns recorded on samples obtained at pH 2 at (a) 350 °C, (b) 450 °C, and (c) 750 °C: (●) $(NH_4)_3Fe(SO_4)_3$, (○) $(NH_4)_2SO_4 \cdot Fe_2(SO_4)_3$, (▲) $NH_4Fe(SO_4)_2$, (▨) αFe_2O_3, (⊡) $Fe_{12}O_3(SO_4)_{15}$, (▽) $Fe_2(SO_4)_3$.

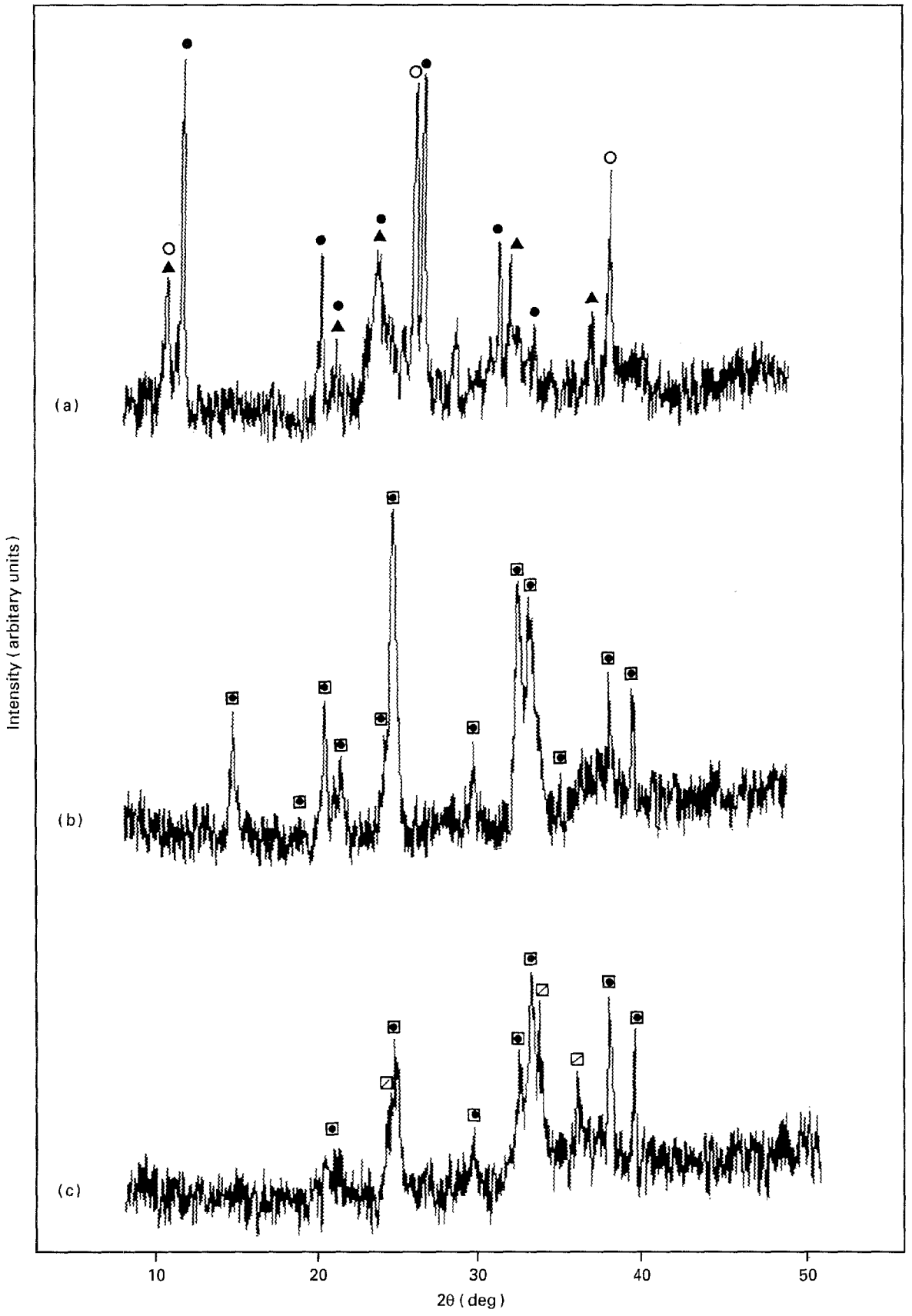

Figure 4 X-ray high temperature powder diffraction patterns recorded on samples obtained at pH 2 analysed at (a) 275 °C, (b) 375 °C, and (c) 500 °C: (●) $(NH_4)_3Fe(SO_4)_3$; (○) $(NH_4)_2SO_4 \cdot Fe_2(SO_4)_3$, (▲) $NH_4Fe(SO_4)_2$, (▨) αFe_2O_3, (⊡) $Fe_{12}O_3(SO_4)_{15}$.

are seen to be lower than those registered by calorimetry in air.

5. Conclusions

The products obtained from the evaporation–crystallization of bio-oxidized sulphuric water pickling liquors containing ferrous sulphate have been studied and characterized.

Bacterial oxidation carried out in an ammonium containing medium, is conducive to the formation of mono- and triammonium salts and Fe(III) hydroxysalts. The appearance of the latter in the final crystalline product depends upon pH. At pHs of less

TABLE III Estimated values for free energy, ΔG°, corresponding to the possible chemical species present in the studied solution

Species	ΔG° (kcal mol^{-1}) [15]
$Fe_2(SO_4)_3$[a]	− 536.1
$Fe_2(OH)_2^{4+}$[a]	− 111.7
$Fe(SO_4)_2^-$[a]	− 294.8
$Fe(OH)_3$	− 168.6
$Fe(OH)_3$[a]	− 119.8

[a] Indicates in solution.

than two, Fe(III) hydroxysalts are not formed and the monoammonium salt $(NH_4)Fe(SO_4)_2$ is the only salt found in the oxidized solution. When the solution is evaporated and crystallized, the triammonium salt $(NH_4)_3Fe(SO_4)_3$ also forms as a consequence of reaction between the majority monoammonium salt and ammonium and sulphate ions present in the solution. The concentration of this triammonium salt increases with increasing pH and becomes the major product obtained when the solution is oxidized at pH 2 followed by evapo–crystallization. At this pH, Fe(III) hydroxysalts are also formed, as well as the double salt $(NH_4)_2SO_4 \cdot Fe_2(SO_4)_3$. This is formed during the evaporation of the solution, probably by a reaction (chemical, physical retention or occlusion) between crystallized ferric sulphate and ammonium sulphate produced during the progressive concentrating of ammonium and sulphate ions throughout the evaporation process. Small quantities of hydroniojarosite are also found under these conditions.

Finally, the results provide interesting data with respect to the thermal decomposition of these compounds in air. The results allow the establishment of the decomposition temperatures of the compounds studied. Further, they provide information on their infrared absorption patterns.

Acknowledgements

We thank the European Community 7261/02/512 Convention (Research Programme "Technical Control of Nuisances and Pollution in the Workplace and in the Environment of Iron and Steel Works") for the financial support enabling us to carry out this research.

References

1. J. O. BURCKLE and H. M. FREEMAN, in "Proceedings of Iron Control in Hydrometallurgy", edited by E. Horwood, Chichester, 1986, p. 754.
2. F. J. GARCIA, A. RUBIO, E. SAINZ, P. GONZALEZ and F. A. LOPEZ, *FEMS Microb. Rev.* **14** (1994) 397.
3. F. A. LOPEZ, F. J. GARCIA, A. RUBIO and P. GONZALEZ, in Report 7261/02/512 of Commission of the European Communities, July 1994.
4. C. A. SCHNAITMAN, M. S. KORCZYNSKI and D. G. LUNDGREN, *J. Bacteriol.* **99** (1969) 552.
5. J. L. BARRON and D. R. LUEKING, *Appl. Environ. Microbiol.* **56** (1990) 2801.
6. L. TORO, R. de SANTIS, M. PELINO, N. M. IVAGNES and C. CANTALINI, "Fundamental and applied biohydrometallurgy" (Elsevier, Amsterdam, 1986) pp. 476–478.
7. K. C. IVARSON, G. J. ROSS and N. M. MILLES, *Soil Sci. Soc. Amer.* **43** (1979) 908.
8. N. LAZAROFF, W. SIGAL and A. WASSERMAN, *Appl. Environ. Microbiol.* **43** (1982) 924.
9. M. P. SILVERMAN and D. G. LUNDGREN, *J. Bacteriol.* **77** (1959) 642.
10. C. J. SERNA, C. PARADA and J. V. GARCIA RAMOS, *Spectrochim. Acta* **42A** (1986) 729.
11. S. LOPEZ ANDRES, "Cristaloquimica y propiedades físicoquímicas de materiales tipo jarosita", (Universite Complutense, Madrid, 1987).
12. D. A. POWERS, G. R. ROSSMAN, H. J. SHUGAR and H. B. GRAY, *J. Solid State Chem.* **13** (1975) 1.
13. M. M. SHOKAREV, E. V. MARGULIS, F. I. VERSHININA, L. I. BEISEKEEVA and L. A. SAVCHENKO, *Russ. J. Inorg. Chem.* **17** (1972) 1293.
14. M. FOLDVARI, F. PAULIK and J. PAULIK, *J. Thermal Anal.* **33** (1988) 121.
15. Outokumpu Research, "Chemical Reaction and Equilibrium Software" (1992).

Received 22 December 1994
and accepted 2 May 1995